

Short-range correlations in the electron gas

Kevin Bedell and G. E. Brown

Nordita, Blegdamsvej 17, DK-2100 Copenhagen Ø, Denmark
and Physics Department, State University of New York, Stony Brook, New York 11794

(Received 18 October 1977)

The effects of short-range correlations on the properties of the electron gas are studied using an approach phrased in the polarization potential language of Pines and Nozières. It was argued by Lowy and Brown that two-body terms make up the dominant contribution to the effective interaction for large momentum transfers. In the region of small-momentum transfers it is known that the random-phase approximation provides an adequate picture of the electron gas. With these two regions of large- and small-momentum transfers in mind, a polarization propagator is constructed to interpolate between them. A number of sum rules, among them the f -sum rule, involving the imaginary part of the polarization propagator, were found to be satisfied. The failure of our theory to satisfy the compressibility sum rule is discussed in detail. We present here the results for the local t -matrix, the dynamic and static form factors, and the pair correlation function. That our pair-correlation function remains positive and is essentially the same as in the paper of Lowy and Brown indicates that the physics and not the formalism is responsible for the results we obtain.

I. INTRODUCTION

In a series of papers,¹ Singwi and collaborators developed a method for inclusion of short-range correlations in the electron gas at metallic densities. The method was somewhat intuitive, making a conjecture for the behavior of the density-density correlation function at small separations, and then iterating the relevant equations to achieve self-consistency. In later work, Lowy and Brown² showed that summation of ladder diagrams of the Coulomb interaction reproduced numerically the results of Singwi *et al.* They adduced arguments to make it plausible that for small separations (large-momentum transfers), such a summation dominated the effective interaction between electrons in the electron gas. For large separations (small-momentum transfers), it is known that the random-phase approximation (RPA) is a good approximation. With these two limiting values of the effective interaction, an effective interaction was constructed that interpolated between the large- and small-momentum-transfer regions.

With this effective interaction various properties of the electron gas were studied. One of the quantities studied was the pair-correlation function, $g(r)$ at metallic densities. The method employed by Lowy and Brown in their paper was borrowed from the Brueckner theory of nuclear matter. A correlated wave function was constructed from the effective interaction and $g(r)$ was computed from this wave function. An important result of this calculation was that $g(r)$ remained positive for all $r \geq 0$ and for all densities studied. This in itself is an important result since all other approximations give negative values for the pair-

correlation function at small separations at densities in which $r_s \geq 5$.

The results they obtained for $g(r)$ were somewhat unclear. The pair-correlation function was obtained from the squared absolute value of the correlated wave function which is positive by definition. Thus, the exact comparison with other methods of building short-range correlations into the effective interaction were obscured by the method used in obtaining $g(r)$.

In this paper, we use a more conventional approach, phrased in the polarization-potential language closely related to that of Pines and Nozières³ and Aldrich *et al.*,⁴ to study the properties of electrons in the electron gas. Our approach in this paper is to construct a density-density response function (polarization propagator) in which the bare Coulomb interaction is replaced by a local average of the ladder diagrams which includes both direct and exchange terms. This, we will see, takes into account in an approximate way the contributions arising from the proper polarization diagrams, some of which are shown in Fig. 4. We find using this approach that the results we obtain for the pair-correlation function are essentially the same as those of Lowy and Brown (LB). Since the two approaches are different and the results are the same, we feel confident in our claim that it is the physics that keeps $g(\vec{r})$ positive and that it is not due to some artifact of the method used to construct $g(\vec{r})$.

In addition to the pair-correlation function, we give the numerical results for: the local t matrix, the dynamic form factor $S(\vec{q}, \omega)$, and the static form factor $S(\vec{q})$. A discussion of sum rules and other checks of consistency are given in Sec. IV.

II. t MATRIX

In Sec. II A, we will discuss the construction of our effective interaction which interpolates between the large- and small-momentum transfer regions. In Sec. II, we outline the arguments given in LB for retaining only the ladder diagrams for the effective interactions at short distances, and in detail the numerical methods used in constructing a local t matrix.

A. Short-range interaction

The long-range part of the effective interaction of electrons in an electron gas is screened. The distance scale for screening is essentially governed by the reciprocal of the Fermi-Thomas momentum q_{FT} . For electrons that come closer than this typical distance, the effects of screening become negligible. This decrease in the screening is mainly due to two phenomena: (i) the repulsive nature of the interaction and (ii) the fact that electrons are spin- $\frac{1}{2}$ fermions.

If two electrons are close together, it costs a considerable amount of energy to bring a third electron near the pair of electrons since the third one must approach a double charge. To screen the interaction between two electrons a third electron must be introduced. Since the energy of introducing a third electron is large, we have from the uncertainty principle that the lifetime of this virtual state of three electrons is short, compared to the lifetime of the electron pair.

We have an additional decrease in the screening due to exchange cancellations. If we have three electrons close together at least two of the electrons will have their spins parallel. Because of the Pauli principle, this will cause a further reduction in the screening, expressed as a cancellation of the direct and exchange screening in our formalism. In LB it was shown that this cancellation was of the order k_F^2/q^2 . Denoting the term corresponding to Fig. 1(a) by D_a , etc., they showed that for $q > k_F$, each of the ladder diagrams were of the same order in k_F/q ,

$$D_b/D_a = 0.165r_s [1 + O(k_F^2/q^2)]. \quad (1)$$

If only direct screening terms were kept, they found that

$$D_c/D_a = 0.110r_s (k_F^4/q^4) [1 + O(k_F^2/q^2)]. \quad (2)$$

This, however, overestimates the screening since including the exchange term Fig. 1(d) gives

$$(D_c + D_d)/D_a = 0.880r_s (k_F^6/q^6) [1 + O(k_F^2/q^2)]. \quad (3)$$

Since the long-range part of the interaction will include the effects of screening and at short ranges

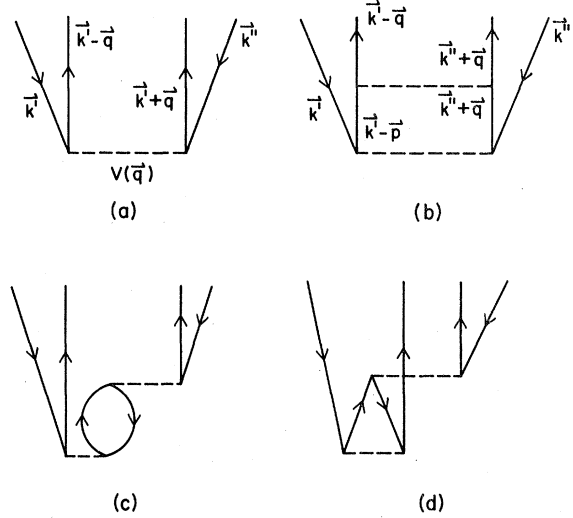


FIG. 1. For $q > k_F$ first- and second-order ladder contributions (a) and (b) are the same order in k_F/q . Second-order direct screening term (c) is order k_F^4/q^4 smaller than (a) or (b), but (c) plus the exchange screening term (d) is order k_F^6/q^6 smaller than (a) or (b).

the screening is negligible, we do not include screening diagrams for short ranges since this will double count the screening diagrams for long ranges. Thus, we restrict our short-range piece of the interaction to be the sum to all orders of ladder diagrams in the unscreened Coulomb potential.

B. Particle-particle t matrix

In studying the scattering of two electrons it is convenient to introduce the t matrix. The t matrix is the solution to the Lippmann-Schwinger integral equation which formally sums to all orders the ladder diagrams of Fig. 2. We can write this equation in momentum space in terms of the relative and center of mass momentum \vec{p} and \vec{K} where $\vec{p} = \frac{1}{2}(\vec{k}_1 - \vec{k}_2)$ and $\vec{K} = \vec{k}_1 + \vec{k}_2$. If the system scatters from an initial state $|\vec{p}, \vec{K}\rangle$ to the final state $|\vec{p}', \vec{K}'\rangle$ (where both states are plane-wave states in the relative and center of mass momentum) the t matrix can be written in the following way:

$$\begin{aligned} \langle \vec{p}', \vec{K}' | t(E) | \vec{p}, \vec{K} \rangle &= \langle \vec{p}' | V | \vec{p} \rangle + \int \frac{d^3k}{(2\pi)^3} \langle \vec{p}' | V | \vec{k} \rangle \\ &\times \frac{1}{E - \epsilon(\frac{1}{2}\vec{K}' + \vec{k}) - \epsilon(\frac{1}{2}\vec{K} - \vec{k})} \\ &\times \langle \vec{k} \vec{K}' | t(E) | \vec{p}, \vec{K} \rangle, \end{aligned} \quad (4)$$

where

$$\langle \vec{p}' | V | \vec{p} \rangle = \lim_{\eta \rightarrow 0} \frac{4\pi e^2}{|\vec{p}' - \vec{p}|^2 + \eta^2}. \quad (5)$$

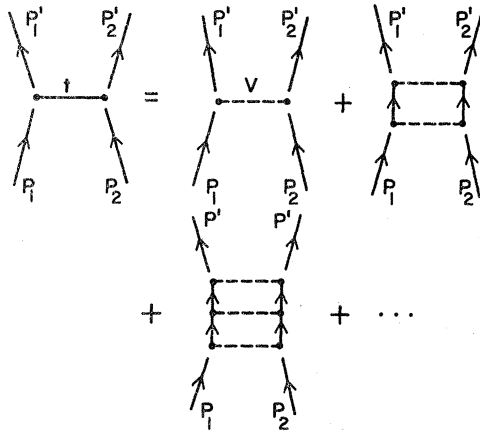


FIG. 2. t matrix of Eq. (4) formally sums to all orders diagrams of this type. If we restrict the intermediate momenta to be greater than k_F we have the diagrams that are summed by Eq. (7).

The energies $\epsilon_{|\vec{p}|}$ are the single-particle energies which for free electrons are given by $\epsilon_{|\vec{p}|} = p^2/2m$. The energy E is just the initial energy of the two-particle state

$$E = \epsilon_{|\frac{1}{2}\vec{K} + \vec{p}|} + \epsilon_{|\frac{1}{2}\vec{K} - \vec{p}|}. \quad (6)$$

The units are chosen such that $\hbar = 1$, $1/m = 7.619$ eV \AA^2 , and $4\pi e^2 = 181.018$ eV \AA .

In the presence of a many-body medium, the interaction of the two electrons will be modified. From now on, we are interested only in the short-range piece of our interaction. In this region, it was shown that only the two-body terms will dominate and that higher-order terms involving the screening of the interaction can be neglected. We can approximate this by treating the many-body medium as a filled Fermi sea of noninteracting electrons whose only role is to restrict the intermediate momenta of the interacting pair of electrons. The initial state of the two electrons is such that $0 \leq |\frac{1}{2}\vec{K} \pm \vec{p}| \leq k_F$; thus, all transitions to states above the Fermi sea are virtual and no real transitions occur.

The presence of the filled Fermi sea restricts the intermediate momenta to be above the Fermi momentum k_F . To take into account the restriction on the intermediate momenta in Eq. (4), we introduce the Pauli projection operator $Q(\vec{k}, \vec{K}, k_F)$ into the kernel of the integral of Eq. (4),

$$\begin{aligned} \langle \vec{p}', \vec{K} | t(E) | \vec{p}, \vec{K} \rangle &= \langle \vec{p}' | V | \vec{p} \rangle + \int \frac{d^3k}{(2\pi)^3} \langle \vec{p}' | \vec{V} | k \rangle \frac{Q(\vec{k}, \vec{K}, k_F)}{E - \epsilon_{|\frac{1}{2}\vec{K} + \vec{k}|} - \epsilon_{|\frac{1}{2}\vec{K} - \vec{k}|}} \\ &\quad \times \langle \vec{k}, \vec{K} | t(E) | \vec{p}, \vec{K} \rangle, \end{aligned} \quad (7)$$

where

$$\begin{aligned} Q(\vec{k}, \vec{K}, k_F) &= \Theta(|\frac{1}{2}\vec{K} + \vec{k}| - k_F) \Theta(|\frac{1}{2}\vec{K} - \vec{k}| - k_F), \\ \Theta(k) &= \begin{cases} 1, & \text{if } k > 0 \\ 0, & \text{if } k \leq 0. \end{cases} \end{aligned} \quad (8)$$

Equation (7) is identical to the Brueckner G matrix of nuclear matter calculations which sums to all orders the ladder diagrams of Fig. 2 where all intermediate states are particles, i.e., $k > k_F$. In our approximation we ignore self-energy corrections to the single-particle excitation spectrum and use only the free-particle spectrum for our energies; thus, $\epsilon_{|\vec{p}|} = p^2/2m$. This approximation may not be valid in light of the recent experimental work in the region of large-momentum transfers.⁵⁻⁷ It does, however, account for some of the features of these experiments. We shall not go into the details of the experimental findings in this paper, but we will refer to them and compare some of our results with them in this paper. The energy denominator of Eq. (7) in this approximation reduces to $(p^2 - k^2)/m$.

In Sec. IIC we construct a particle-hole t matrix from the particle-particle t matrix. For this we must include exchange corrections in the t matrix. This is most simply done when the t matrix is expanded in a partial-wave series. To perform the partial-wave decomposition of the t matrix we must approximate the Pauli operator by its angle average \bar{Q} ,⁸

$$\int d\Omega_{\vec{k}} Q(\vec{k}, \vec{K}, k_F) = \bar{Q}(k, K, k_F) \int d\Omega_{\vec{k}} \vec{k}, \quad (9)$$

thus,

$$\bar{Q}(k, K, k_F) = \begin{cases} 0, & k^2 + \frac{1}{4}K^2 < k_F^2 \\ 1, & |k - \frac{1}{2}K| > k_F \\ \frac{k^2 + \frac{1}{4}K^2 - k_F^2}{kK}, & \text{otherwise} \end{cases} \quad (10)$$

If we use \bar{Q} in Eq. (7) t becomes a function only of the magnitude of K . The only angle we have left to expand in is the angle between the initial and final relative momentum. In terms of partial waves, we can write the t matrix as follows:

$$\begin{aligned} \langle \vec{p}' | t^K(E) | \vec{p} \rangle &= 4\pi \sum_{l=0}^{\infty} (2l+1) \langle p' | t_l^K(E) | p \rangle P_l(\hat{p}' \cdot \hat{p}). \end{aligned} \quad (11)$$

We can also expand the Coulomb interaction in this angle,

$$\langle p' | V | p \rangle = 4\pi \sum_{l=0}^{\infty} (2l+1) \langle p' | V_l | p \rangle P_l(\hat{p}' \cdot \hat{p}), \quad (12)$$

where

$$\langle p' | V_l | p \rangle = \lim_{n \rightarrow 0} \frac{e^2}{2p'p} Q_l \left(\frac{p'^2 + p^2 + n^2}{2pp'} \right). \quad (13)$$

The functions P_l and Q_l are just the Legendre functions of the first and second kind.

If we plug Eqs. (11) and (12) into Eq. (7) and replace Q by \bar{Q} the integral equation decouples into integral equations for each partial wave,

$$\begin{aligned} \langle p' | t_l^K | p \rangle &= \langle p' | V_l | p \rangle \\ &+ \frac{2m}{\pi} \int_0^\infty dk k^2 \langle p' | V_l | k \rangle \\ &\times \frac{\bar{Q}(k, K, k_F)}{p^2 - k^2} \langle k | t_l^K | p \rangle. \end{aligned} \quad (14)$$

C. Particle-hole t matrix

Using the Pauli operator in Eq. (7) is equivalent to antisymmetrizing the wave function of the interacting pair of electrons with respect to the filled Fermi sea of noninteracting electrons. We must also antisymmetrize the wave function of the interacting pair of electrons. To compute matrix elements of the interaction we need only antisymmetrize the front or the back wave functions. The two lowest-order diagrams that are included in the particle-particle t matrix are shown in Fig. 3(a). We note that the antisymmetrization of the wave function takes into account the exchange contribution to the interaction. The matrix elements for the direct v_d and the exchange v_e terms are

$$V_d = \langle \vec{k}_1 - \vec{q}, \vec{k}_2 | V | \vec{k}_1, \vec{k}_2 - \vec{q} \rangle, \quad (15a)$$

$$V_e = \langle \vec{k}_2, \vec{k}_1 - \vec{q} | V | \vec{k}_1, \vec{k}_2 - \vec{q} \rangle. \quad (15b)$$

We can use these two lowest-order elements of the particle-particle interaction to construct the lowest-order particle-hole matrix element⁹ V_{ph} , where

$$V_{ph} = \langle \vec{k}_2 - \vec{q}, \vec{k}_2 | V_{ph} | \vec{k}_1 - \vec{q}, \vec{k}_1 \rangle. \quad (16a)$$

In terms of the particle-particle matrix elements we can write this in the following way:

$$\begin{aligned} V_{ph} &= \langle \vec{k}_1 - \vec{q}, \vec{k}_2 | V | \vec{k}_1, \vec{k}_2 - \vec{q} \rangle \\ &- \langle \vec{k}_2, \vec{k}_1 - \vec{q} | V | \vec{k}_1, \vec{k}_2 - \vec{q} \rangle \end{aligned} \quad (16b)$$

The diagrams for the particle-hole matrix element in lowest order are shown in Fig. 3(b).

The partial wave decomposition of the t matrix allows us to construct, in a simple way, a particle-hole t matrix which takes into account both the direct and exchange contributions to the interaction. Note that since the exchange term is included, particle-hole ladders are also summed in

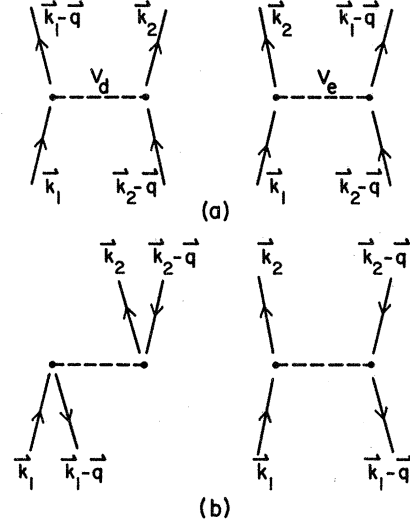


FIG. 3. In (a), we have the lowest-order particle-particle direct and exchange matrix elements. The diagrams in (b) are just the lowest-order particle-hole direct and exchange matrix elements.

our theory. In our final results they are included only approximately, however, because of our need to average over the Fermi sea to obtain a local t matrix, as discussed in Sec. II E. The wave function of the incoming or outgoing states must be antisymmetric in both the spin and coordinate space. If they are in a spin singlet state, only the even partial waves will contribute with a weight of $\frac{1}{2}$ to the interaction. If they are in a spin triplet state, only the odd partials will contribute and they will have a weight of $\frac{3}{2}$. The particle-hole t matrix is obtained from Eq. (16b) by replacing each V by a t . If we write this in terms of the relative and center of mass momentum and denote the particle-hole t matrix by $t_{ph}^K(p', p)$ then,

$$\begin{aligned} t_{ph}^K(p', p) &= 4\pi \sum_{l=\text{odd}} \frac{3}{2}(2l+1) \langle p' | t_l^K | p \rangle P_l(\hat{p}' \cdot \hat{p}) \\ &+ 4\pi \sum_{l=\text{even}} \frac{1}{2}(2l+1) \langle p' | t_l^K | p \rangle P_l(\hat{p}' \cdot \hat{p}). \end{aligned} \quad (17)$$

D. Numerical methods

It is well known that the Coulomb interaction has an infinite range. In momentum space this appears as a divergence of the interaction in the limit of small-momentum transfers. In this limit of small-momentum transfers, many partial waves will contribute to the interaction. This same behavior will persist for small-momentum transfers in the t matrix. In the original program the t matrix was evaluated directly by solving for each partial wave using Eq. (14) and then they were plugged into Eq. (17) to give the t matrix. This

required a considerable amount of computer time since a large number of partial waves were required for small-momentum transfers. Instead of this direct approach, we used a modified approach suggested by Alpo Kallio.¹⁰

Symbolically, we can write Eq. (14)

$$t_i = V_i + V_i(Q/\epsilon)t_i,$$

where

$$\epsilon = E - \epsilon_{|\frac{1}{2}\vec{k} + \vec{k}_i} - \epsilon_{|\frac{1}{2}\vec{k} - \vec{k}_i}.$$

If we let $t_i = v_i + \tilde{t}_i$ then,

$$\begin{aligned} V_i + \tilde{t}_i &= V_i + V_i(Q/\epsilon)(V_i + \tilde{t}_i), \\ \tilde{t}_i &= V_i(Q/\epsilon)V_i + V_i(Q/\epsilon)\tilde{t}_i. \end{aligned} \quad (18)$$

Equation (18) is now an integral equation for the new quantity \tilde{t}_i . We can write this as follows

$$(1 - V_i(Q/\epsilon))\tilde{t}_i = V_i(Q/\epsilon)V_i.$$

Inverting the integral operator on the left yields

$$\tilde{t}_i = (1 - V_i(Q/\epsilon))^{-1}V_i(Q/\epsilon)V_i. \quad (19)$$

Equation (19) is a matrix equation for \tilde{t}_i in which the rows and columns are labeled by the initial and final relative momentum defined on a set of Gauss points. Since all quantities on the right-hand side of Eq. (19) are known, this yields an exact result for \tilde{t}_i (except for the errors arising from the Gaussian quadrature methods used and other errors of a numerical nature).

The usefulness of this approach is that for small-momentum transfers \tilde{t}_i is a small finite quantity. The divergence at small momenta of the t matrix comes from the v_i 's in Eq. (14). To construct the particle-hole t matrix from the partial-wave series of Eq. (17), many v_i 's are needed, however, the computing time for these is very small. If we replace the t_i^K of Eq. (17) by $v_i + \tilde{t}_i$, we have the following equation:

$$\begin{aligned} t_{ph}^K(p', p) &= 4\pi \sum_{l=\text{odd}} \frac{3}{2}(2l+1) \langle p' | V_l | p \rangle P_l(\hat{p}' \cdot \hat{p}) \\ &+ 4\pi \sum_{l=\text{even}} \frac{1}{2}(2l+1) \langle p' | V_l | p \rangle P_l(\hat{p}' \cdot \hat{p}) \\ &+ 4\pi \sum_{l=\text{odd}} \frac{3}{2}(2l+1) \langle p' | \tilde{t}_l^K | p \rangle P_l(\hat{p}' \cdot \hat{p}) \\ &+ 4\pi \sum_{l=\text{even}} \frac{1}{2}(2l+1) \langle p' | \tilde{t}_l^K | p \rangle P_l(\hat{p}' \cdot \hat{p}). \end{aligned} \quad (20)$$

The sum over the v_i 's requires many terms, but they are easy to compute. The sum over the \tilde{t}_i 's requires very few terms and thus the computing time is considerably reduced from the time it takes using the more direct approach.

E. Local t matrix

In Sec. III, we plan to use our t matrix to construct an RPA-type theory to study the properties of the electron gas at metallic densities. The t matrix we have constructed is a nonlocal operator, however, and would introduce great complications in connection with gauge invariance, etc. Since our arguments show that the effective operator is local at both high and low q , we shall construct a local operator to interpolate between the regions of large- and small-momentum transfers. We have no justification for this operator for intermediate q , $q \sim k_F$. Since the t matrix for large-momentum transfers was a slowly varying function of the relative and center of mass momentum, and for small q it approaches the Coulomb interaction we defined a local particle-hole t matrix, denoted by $t_{ph}^{loc}(q)$, as follows:

$$\begin{aligned} t_{ph}^{loc}(q) &= \frac{1}{N_{av}} \int \frac{d^3k}{(2\pi)^3} \\ &\times \int \frac{d^3K}{(2\pi)^3} [1 - \bar{Q}(k, K, k_F)] t_{ph}^K(k, q), \end{aligned} \quad (21)$$

where

$$N_{av} = \int \frac{d^3k}{(2\pi)^3} \int \frac{d^3K}{(2\pi)^3} [1 - \bar{Q}(k, K, k_F)]. \quad (22)$$

It turns out that the dependence on K was very weak so rather than integrating over K we set K equal to some constant value and integrated over the relative momentum k . We varied K over a wide range of values and found no change in $t_{ph}^{loc}(q)$. In Table I, we list values for our local t matrix for a number of densities. It can be seen that $t_{ph}^{loc}(q)$ deviates from the Coulomb potential, $4\pi e^2/q^2$, only by terms of order q^2/k_F^2 for small q .

III. PROPERTIES OF THE ELECTRON GAS

A. Density-density response function

A quantity of interest in studying the electron gas is the density-density response function (polarization propagator), $\chi(\vec{q}, \omega)$. In general, we can write this in the following way:

$$\chi(\vec{q}, \omega) = \Pi^*(\vec{q}, \omega) / \left(1 - \frac{4\pi e^2}{q^2} \Pi^*(\vec{q}, \omega)\right), \quad (23)$$

where¹¹ $\Pi^*(\vec{q}, \omega) = \sum$ (all proper polarization graphs). (A proper polarization diagram is a polarization diagram that cannot be separated into two polarization diagrams by cutting a single interaction line.) Some of the diagrams included in $\Pi^*(\vec{q}, \omega)$ are shown in Fig. 4. The lowest-order proper polarization diagram Fig. 4(a) is just the

TABLE I. Local t matrix and Coulomb potential (units: $4\pi e^2 = 181 \text{ eV \AA}$).

| r_s | 1 | 2 | 3 | 4 | 5 | | | | | |
|---------|----------------|------------------------|----------------|------------------------|----------------|------------------------|----------------|------------------------|----------------|------------------------|
| q/k_F | t_{ph}^{loc} | $\frac{4\pi e^2}{q^2}$ |
| 0.2 | 338 | 344 | 1348 | 1376 | 3030 | 3097 | 5382 | 5505 | 8401 | 8601 |
| 0.4 | 73.5 | 86.0 | 281 | 344 | 610 | 774 | 1053 | 1376 | 1605 | 2150 |
| 0.6 | 29.8 | 38.2 | 109 | 153 | 231 | 344 | 387 | 612 | 576 | 956 |
| 0.8 | 14.5 | 21.5 | 51.1 | 86.0 | 104 | 193 | 170 | 344 | 246 | 538 |
| 1.0 | 7.71 | 13.8 | 25.9 | 55.1 | 50.6 | 124 | 79.9 | 220 | 112 | 344 |
| 1.2 | 4.36 | 9.56 | 13.8 | 38.2 | 25.3 | 86.0 | 37.6 | 153 | 49.9 | 239 |
| 1.4 | 2.63 | 7.02 | 7.74 | 28.1 | 13.2 | 63.2 | 17.9 | 112 | 21.4 | 175 |
| 1.6 | 1.67 | 5.38 | 4.72 | 21.5 | 7.71 | 48.4 | 10.0 | 86.0 | 11.5 | 134 |
| 1.8 | 1.24 | 4.25 | 3.58 | 17.0 | 6.05 | 38.2 | 8.28 | 68.0 | 10.2 | 106 |
| 2.0 | 0.95 | 3.44 | 2.76 | 13.8 | 4.67 | 31.0 | 6.43 | 55.1 | 7.91 | 86.0 |
| 2.2 | 0.79 | 2.84 | 2.33 | 11.4 | 4.03 | 25.6 | 5.69 | 45.5 | 7.26 | 71.1 |
| 2.4 | 0.69 | 2.39 | 2.06 | 9.56 | 3.64 | 21.5 | 5.27 | 38.2 | 6.89 | 59.7 |
| 2.6 | 0.60 | 2.04 | 1.81 | 8.14 | 3.21 | 18.3 | 4.67 | 32.6 | 6.12 | 50.9 |
| 2.8 | 0.53 | 1.76 | 1.59 | 7.02 | 2.82 | 15.8 | 4.08 | 28.1 | 5.35 | 43.9 |
| 3.0 | 0.47 | 1.53 | 1.42 | 6.12 | 2.51 | 13.8 | 3.65 | 24.5 | 4.79 | 38.2 |
| 3.2 | 0.42 | 1.34 | 1.27 | 5.38 | 2.25 | 12.1 | 3.28 | 21.5 | 4.30 | 33.6 |
| 3.4 | 0.38 | 1.19 | 1.14 | 4.76 | 2.02 | 10.9 | 2.94 | 19.1 | 3.86 | 29.8 |
| 3.6 | 0.34 | 1.06 | 1.03 | 4.25 | 1.83 | 9.56 | 2.66 | 17.0 | 3.50 | 26.5 |
| 3.8 | 0.31 | 0.95 | 0.93 | 3.81 | 1.66 | 8.58 | 2.42 | 15.3 | 3.19 | 23.8 |
| 4.0 | 0.28 | 0.86 | 0.85 | 3.44 | 1.51 | 7.74 | 2.21 | 13.8 | 2.91 | 21.5 |
| 5.0 | 0.18 | 0.55 | 0.55 | 2.20 | 0.97 | 4.95 | 1.41 | 8.81 | 1.85 | 13.8 |
| 6.0 | 0.13 | 0.38 | 0.39 | 1.53 | 0.70 | 3.44 | 1.02 | 6.12 | 1.34 | 9.56 |
| 7.0 | 0.10 | 0.28 | 0.29 | 1.12 | 0.51 | 2.53 | 0.74 | 4.49 | 0.97 | 7.02 |
| 8.0 | 0.07 | 0.22 | 0.22 | 0.86 | 0.39 | 1.94 | 0.56 | 3.44 | 0.73 | 5.38 |

Lindhard function¹² $\Pi_0(\vec{q}, \omega)$,

$$\Pi_0(\vec{q}, \omega) = -2i \int \frac{d^4k}{(2\pi)^4} G_0(\vec{q} + \vec{k}, \omega + k_0) G_0(\vec{k}, k_0), \quad (24)$$

where $G_0(k)$ [k is a four-momentum, $k = (\vec{k}, k_0)$] is just the propagator for a free particle or hole of momentum k ,

$$G_0(k) = \frac{i}{k_0 - \epsilon_{|\vec{k}|} + i\delta \text{sgn}(|\vec{k}| - k_F)},$$

$$\epsilon_{|\vec{k}|} = k^2/2m. \quad (25)$$

Our approximation for $\chi(\vec{q}, \omega)$ involves the following substitutions: We replace $\Pi^*(\vec{q}, \omega)$ in the numerator of Eq. (23) with $\Pi_0(\vec{q}, \omega)$ and the term $(4\pi e^2/q^2)\Pi^*(\vec{q}, \omega)$ is replaced by the expression $t_{ph}^{loc}(q)\Pi_0(\vec{q}, \omega)$. The density-density response function in this theory becomes

$$\chi^{LB}(\vec{q}, \omega) = \Pi_0(\vec{q}, \omega) / [1 - t_{ph}^{loc}(q)\Pi_0(\vec{q}, \omega)]. \quad (26)$$

Since exchange contributions and ladder diagrams summed to all orders have been included in the

local t matrix, we are taking into account in an approximate way some of the diagrams of Fig. 4. This approximation is in keeping with the spirit of the work by Hubbard,¹³ Pines and Nozières,³ Vashishta and Singwi,¹⁴ etc.

Generally, each of these theories, including the one of the present paper, can be cast into the following form:

$$\chi(\vec{q}, \omega) = \frac{\Pi_0(\vec{q}, \omega)}{1 - (4\pi e^2/q^2)[1 - f(q)]\Pi_0(\vec{q}, \omega)}, \quad (27)$$

where $f(q)$ depends on the particular theory. In Hubbard's approximation we have

$$f^H(q) = q^2/2(q^2 + k_F^2). \quad (28)$$

In the theory of Vashishta and Singwi we can write $f(q)$ in terms of their $G(q)$,

$$f^{VS}(q) = G(q). \quad (29)$$

In the LB theory, $f(q)$ is given in terms of the local t matrix,

$$f^{LB}(q) = \frac{(4\pi e^2/q^2) - t_{ph}^{loc}(q)}{4\pi e^2/q^2} = \frac{-q^2}{4\pi e^2} t_{ph}^{loc}(q). \quad (30)$$

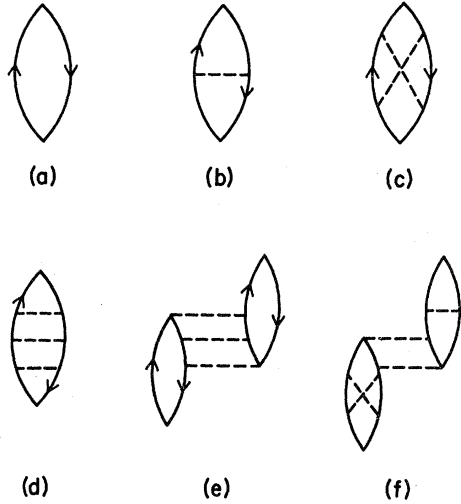


FIG. 4. Typical proper polarization diagrams that are contained in the operator $\Pi^*(q, \omega)$. In our calculation we include the effects of the diagrams (b)–(f), and others like these, in an approximate way.

In the notation of Pines and Nozières,³ $\bar{t}(q)$ is the polarization potential. In Table II, some values for $f^{\text{LB}}(q)$, $f^{\text{VS}}(q)$, and $f^{\text{H}}(q)$ are given. In the approximations of Vashishta and Singwi, and Hubbard, $f(q)$ tends monotonically to an asymptotic value, whereas, in the LB theory, $f(q)$ reaches a maximum at $q = 2k_F$ and then drops off approaching asymptotically to some finite value.

It should be noted that $(4\pi e^2/q^2)f^{\text{LB}}(q)$, or any of the other polarization potentials considered, should be of short range in coordinate space. From Table II it can be seen that $\bar{t}_{ph}^{\text{loc}}(q)$ [see Eq. (30)] must be of order q^2/k_F^2 ($q \ll k_F$) compared with the Coulomb potential. This $(4\pi e^2/q^2)f^{\text{LB}}(q)$ is then our representation of the Pines polarization potential, which is meant to stimulate the Landau f function for neutral systems (see the discussion in Pines and Nozières³).

It can be argued that our neglect of the frequency dependence in our polarization potential is unjustified. Certainly, for intermediate q , $q \sim k_F$, this is so. On the other hand, for very large q , the interacting particles are close together, and the interaction is essentially instantaneous. For small q , our theory goes over into the random-phase approximation, which is known to be good in this region.

B. Dielectric response function and plasmons

Once we are given the density-density response function we can construct a generalized dielectric response function. The two functions are related as follows³

$$\epsilon^{-1}(\vec{q}, \omega) = 1 + (4\pi e^2/q^2)\chi(\vec{q}, \omega). \quad (31)$$

Substituting the expression for $\chi(\vec{q}, \omega)$ in Eq. (23) into Eq. (31) we have that

$$\begin{aligned} \epsilon^{-1}(\vec{q}, \omega) &= 1 + \frac{4\pi e^2}{q^2} \left(\frac{\Pi^*(\vec{q}, \omega)}{1 - (4\pi e^2/q^2)\Pi^*(\vec{q}, \omega)} \right) \\ &= \frac{1}{1 - (4\pi e^2/q^2)\Pi^*(\vec{q}, \omega)}. \end{aligned}$$

Thus, in general the dielectric function can be written as follows:

$$\epsilon(\vec{q}, \omega) = 1 - (4\pi e^2/q^2)\Pi^*(\vec{q}, \omega). \quad (32)$$

In our approximation, the dielectric function becomes

$$\epsilon^{\text{LB}}(\vec{q}, \omega) = 1 - t_{ph}^{\text{loc}}(q)\Pi_0(\vec{q}, \omega). \quad (33)$$

In RPA the dielectric function is given by

$$\epsilon^{\text{RPA}}(\vec{q}, \omega) = 1 - (4\pi e^2/q^2)\Pi_0(\vec{q}, \omega). \quad (34)$$

In the RPA it is well known that for momenta q smaller than some typical cutoff momentum q_c

TABLE II. Values for the functions $f(q)$ defined in the paper.

| q/k_F | 1 | | | 2 | | | 3 | | | 4 | | | 5 | | |
|---------|--------------|--------------|-------------|--------------|--------------|-------------|--------------|--------------|-------------|--------------|--------------|-------------|--------------|--------------|-------------|
| | LB $f(q)$ | VS $f(q)$ | H $f(q)$ |
| 0.2 | 0.02 | 0.01 | 0.02 | 0.02 | 0.01 | 0.02 | 0.02 | 0.01 | 0.02 | 0.02 | 0.01 | 0.02 | 0.02 | 0.01 | 0.02 |
| 0.4 | 0.15 | 0.04 | 0.07 | 0.18 | 0.04 | 0.07 | 0.21 | 0.04 | 0.07 | 0.23 | 0.05 | 0.07 | 0.25 | 0.05 | 0.07 |
| 1.0 | 0.44 | 0.22 | 0.25 | 0.53 | 0.24 | 0.25 | 0.59 | 0.25 | 0.25 | 0.64 | 0.26 | 0.25 | 0.67 | 0.27 | 0.25 |
| 1.4 | 0.63 | 0.37 | 0.33 | 0.72 | 0.41 | 0.33 | 0.79 | 0.44 | 0.33 | 0.84 | 0.47 | 0.33 | 0.88 | 0.49 | 0.33 |
| 2.0 | 0.72 | 0.54 | 0.40 | 0.80 | 0.62 | 0.40 | 0.85 | 0.68 | 0.40 | 0.88 | 0.72 | 0.40 | 0.91 | 0.76 | 0.40 |
| 3.0 | 0.69 | 0.64 | 0.45 | 0.77 | 0.75 | 0.45 | 0.82 | 0.84 | 0.45 | 0.85 | 0.90 | 0.45 | 0.87 | 0.95 | 0.45 |
| 6.0 | 0.66 | 0.71 | 0.49 | 0.75 | 0.85 | 0.49 | 0.80 | 0.95 | 0.49 | 0.83 | 1.01 | 0.49 | 0.86 | 1.05 | 0.49 |
| 8.0 | 0.68 | 0.73 | 0.49 | 0.74 | 0.87 | 0.49 | 0.80 | 0.96 | 0.49 | 0.84 | 1.03 | 0.49 | 0.86 | 1.06 | 0.49 |

there exists a collective mode of the electron gas called a plasmon. This mode appears as a pole in the polarization propagator or as a zero of the dielectric function. In the RPA a dispersion relation for the plasmons can be derived from the condition that

$$\epsilon(\vec{q}, \omega_q) = 0. \quad (35)$$

This, of course, only holds as long as there is no damping, since damping of the plasmon tends to smooth out the pole in $\chi(\vec{q}, \omega)$; thus, $\epsilon(\vec{q}, \omega)$ will have no real zeroes. For small-momentum transfers we find, in the RPA, that

$$\omega_q \simeq \omega_p \left[1 + \frac{3}{5} \left(\frac{q k_F / m}{\omega_p} \right)^2 \right]^{1/2}. \quad (36)$$

We can express this in terms of a dimensionless parameter β which depends on the density and the momentum transfer q' measured relative to k_F (k_F is the Fermi momentum and $\epsilon_F = k_F^2 / 2m$ is the Fermi energy),

$$\omega_q \simeq 2\beta\epsilon_F \left[1 + \frac{3}{5} (q'/\beta)^2 \right]^{1/2},$$

where

$$\omega_p = \frac{4\pi\rho e^2}{m}, \quad \beta = 0.470 r_s^{1/2},$$

and

$$\omega_p = 2\beta\epsilon_F. \quad (36a)$$

The quantity r_s is a dimensionless measure of the average interparticle spacing defined by the relation

$$k_F^3 / 3\pi^2 = 1 / \frac{4}{3} \pi r_0^3. \quad (36b)$$

If we let $r_0 = r_s a_0$ where a_0 is the Bohr radius, $a_0 = 0.5292 \text{ \AA}$, then

$$r_s = \left(\frac{9}{4} \pi \right)^{1/3} / a_0 k_F = 1.919 / a_0 k_F. \quad (36c)$$

The cutoff momentum q_c , i.e., the momentum value for which strong Landau damping occurs, is defined by the set of equations in which³

$$\epsilon(q_c, \omega_{q_c}) = 0,$$

and

$$\omega_{q_c} = q_c k_F / m + q_c^2 / 2m. \quad (37)$$

Solving for q_c' ($q_c' = q_c / k_F$) we have

$$q_c' \simeq 0.470 r_s^{1/2}. \quad (37a)$$

In the LB theory, there exist plasmons whose dispersion relation is found by solving Eq. (35), where we use our dielectric response function defined in Eq. (33). In terms of the dimensionless parameters of Eq. (36a) we have

$$\omega_q^{\text{LB}} = 2\beta\epsilon_F \left[1 + (q'/\beta)^2 \left(\frac{3}{5} + \gamma\beta^2 \right) \right]^{1/2}, \quad (38)$$

where γ was found to range between the values² -0.51 and -0.58 over a range of densities such that, $2 \leq r_s \leq 5$. The cutoff momentum for our theory will be lower than in the RPA. The cutoff momentum is the momentum transfer at which the quasiparticle-hole excitation energy is equal to the plasmon energy and thus Landau damping can occur. Since our plasmons are lower in energy than the plasmons in the RPA, our cutoff momentum will lie below the cutoff of RPA.

We can obtain the cutoff momentum in the LB theory by solving Eq. (37). However, it turns out that we can determine the cutoff q_c' by parametrizing it in the following way:

$$q_c' \simeq a r_s^{1/b}.$$

This was fitted to the momentum value at which the plasmons merged with the particle-hole continuum. This gave for q_c' the value

$$q_c' \simeq 0.438 r_s^{1/3}. \quad (39)$$

This works well in the density range $1 \leq r_s \leq 5$. Note, however, that this discussion depends upon the q^2 term in ω_q , which is determined by the low- q behavior of the corrections to the unscreened Coulomb interaction in our effective interaction, and we have no arguments that these are correctly described. (See our discussion of the compressibility in Sec. IV.)

C. Effective interaction

With our dielectric function we can construct our effective interaction which interpolates between both the large- and small-momentum transfer regions. The effective interaction denoted by $t_{\text{eff}}(\vec{q}, \omega)$ is given by

$$t_{\text{eff}}(\vec{q}, \omega) = t_{ph}^{\text{loc}}(\vec{q}) / \epsilon^{\text{LB}}(\vec{q}, \omega). \quad (40)$$

In the limit of small q , we have that

$$t_{ph}^{\text{loc}}(\vec{q}) \xrightarrow{q \rightarrow 0} 4\pi e^2 / q^2,$$

and

$$\epsilon^{\text{LB}}(\vec{q}, \omega) \xrightarrow{q \rightarrow 0} \epsilon^{\text{RPA}}(\vec{q}, \omega) = 1 - \frac{4\pi e^2}{q^2} \Pi_0(\vec{q}, \omega).$$

Thus, in the small- q limit our effective interaction reduces to the RPA effective interaction

$$t_{\text{eff}}(\vec{q}, \omega) \rightarrow v_{\text{eff}}^{\text{RPA}}(\vec{q}, \omega) = \frac{4\pi e^2 / q^2}{\epsilon^{\text{RPA}}(\vec{q}, \omega)}. \quad (41)$$

In the large- q limit,¹⁵

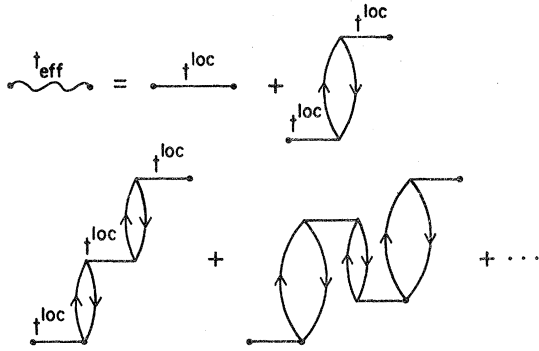


FIG. 5. Our effective interaction formally sums to all orders diagrams of the type shown here.

$$\Pi_0(\vec{q}, \omega) \xrightarrow{q \rightarrow \infty} |\vec{q}|^{-2}.$$

Furthermore, we know that $t_{ph}^{loc}(\vec{q})$ drops off faster than q^{-2} , thus,

$$\epsilon^{LB}(\vec{q}, \omega) \xrightarrow{q \rightarrow \infty} 1.$$

In this limit, we see that

$$t_{eff}(\vec{q}, \omega) \xrightarrow{q \rightarrow \infty} t_{ph}^{loc}(\vec{q}).$$

This is the result we have claimed in Sec. II will occur for large-momentum transfers, i.e., the effects of screening for large q are negligible and only the ladder sum of unscreened Coulomb interactions will contribute in this limit. Figure 5 shows some of the diagrams contained in our effective interaction.

The diagrammatic expansion of $t_{eff}(\vec{q}, \omega)$ shown in Fig. 5 does not make it clear how much we have built into our effective interaction. We can write an equation for the effective interaction in terms of the proper polarization graphs. The integral equation for this can be written symbolically as

$$t_{eff}(\vec{q}, \omega) = t_{ph}^{loc}(\vec{q}) + t_{ph}^{loc}(\vec{q}) \Pi_0(\vec{q}, \omega) t_{eff}(\vec{q}, \omega). \quad (42)$$

Since the expression $t_{ph}^{loc}(q) \Pi_0(\vec{q}, \omega)$ is an approximation to $(4\pi e^2/q^2) \Pi^*(\vec{q}, \omega)$ we have included, in an averaged sense, the contributions of the diagrams of Fig. 4. From the structure of Eq. (42) we see that our effective interaction has taken into account, only approximately because of our need to average over the Fermi sea, the kinds of diagrams shown in Fig. 6.

D. Dynamic and static form factors

The dynamic form factor $S(\vec{q}, \omega)$ is a quantity that can be directly compared to experiment. $S(\vec{q}, \omega)$ is proportional to the differential, inelastic-scat-

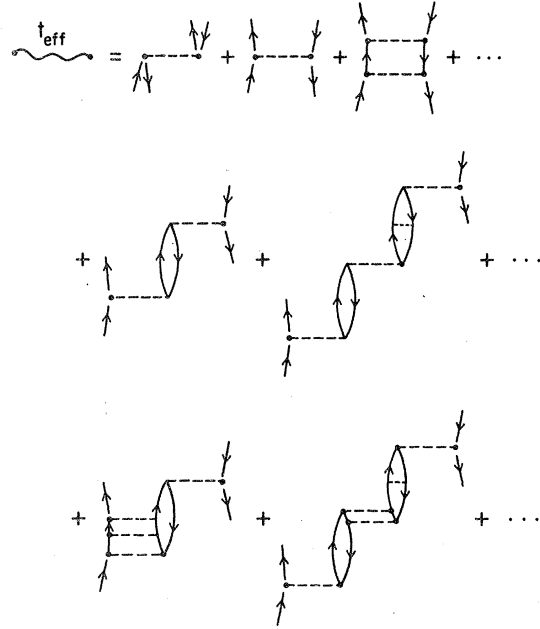


FIG. 6. Diagrams that are included in our effective interaction. Contributions from proper polarization graphs of a higher order than $\Pi_0(q, \omega)$ and graphs with repeated Coulomb interactions are included only approximately.

tering cross sections obtained in energy-loss experiments on solids. The cross section can be written as follows:

$$\frac{d\sigma}{d\Omega} = \sigma S(\vec{q}, \omega). \quad (43)$$

The dynamic form factor contains all of our information about the many-body medium. The cross section σ contains the information about the probe. If the probe is a beam of high-energy electrons, then σ is just the Mott cross section for the scattering of identical particles. For the case of x-ray scattering this is just the Thomson cross section for the scattering of photons off electrons.

The dynamic form factor acts as a spectral density for the density-density response function through the dispersion relation³

$$\chi(\vec{q}, \omega) = \int_0^\infty d\omega' S(\vec{q}, \omega') \left(\frac{1}{\omega - \omega' + i\eta} - \frac{1}{\omega + \omega' + i\eta} \right). \quad (44)$$

If we express $\chi(\vec{q}, \omega)$ in terms of its real and imaginary parts

$$\chi(\vec{q}, \omega) = \text{Re} \chi(\vec{q}, \omega) + i \text{Im} \chi(\vec{q}, \omega),$$

we find that

$$\text{Im} \chi(\vec{q}, \omega) = -\pi [S(\vec{q}, \omega) - S(\vec{q}, -\omega)]. \quad (45)$$

If we assume that the system is initially in its ground state, then $S(\vec{q}, -\omega) = 0$.

The poles of the density-density response function appear as singular structures in the dynamic form factor, for small momenta, at the plasmon frequency. For momentum values below the cutoff momentum q_c we can write the dynamic form factor as a sum of two terms³

$$S(\vec{q}, \omega) = S_{\text{inc}}(\vec{q}, \omega) + S_{\text{pl}}(\vec{q}, \omega). \quad (46)$$

The first term is an incoherent contribution coming from quasiparticle excitations. The second term $S_{\text{pl}}(\vec{q}, \omega)$ is the contribution coming from the plasmon. For $q < q_c$, we can write this as follows:

$$S_{\text{pl}}(\vec{q}, \omega) \approx [|g_q|^2 / V(q)^2] \delta(\omega - \omega_q), \quad (47)$$

where^{16,17}

$$|g_q|^2 = (\omega_p^2 / 2\omega_q) V(q), \quad (47a)$$

and

$$V(q) = 4\pi e^2 / q^2. \quad (47b)$$

The $|g_q|^2$ of Eq. (47a) is the lowest-order expression for the coupling of the plasmons to the particle-hole continuum derived by Dubois.¹⁶ In this region in which $q < q_c$, the term $S_{\text{inc}}(\vec{q}, \omega)$ makes a contribution of the order $(q/k_F)^4$ to $S(\vec{q}, \omega)$ and can be neglected. Thus, for $q < q_c$, $S(\vec{q}, \omega)$ takes on a simple form,

$$S(\vec{q}, \omega) \approx [\omega_p^2 / 2\omega_q V(q)] \delta(\omega - \omega_q). \quad (48)$$

In this paper, we use our dispersion relation for the plasmon frequency given by Eq. (38) for the ω_q that appears in Eq. (48).

The static form factor is obtained from the dynamic form factor by integrating over energy,

$$S(\vec{q}) = \frac{1}{\rho} \int_0^\infty d\omega S(\vec{q}, \omega). \quad (49)$$

The static form factor $S(\vec{q})$ is a measure of the instantaneous density correlations in the system. In terms of the density fluctuation operator ρ_q , $S(\vec{q})$ can be written as

$$\rho S(\vec{q}) = \langle 0 | \rho_q^\dagger \rho_q | 0 \rangle, \quad (50)$$

where $|0\rangle$ is the ground state of the system. We can express ρ_q in terms of the creation a_p^\dagger and annihilation a_p operators in the following way:

$$\rho_q = \sum_p a_{p+q}^\dagger a_p. \quad (51)$$

Thus, $\rho S(\vec{q}, \omega)$ is just the mean-square density fluctuations of the system.

From general arguments, we know that

$$\lim_{q \rightarrow 0} S(\vec{q}) = q^2 / 2m\omega_q. \quad (52)$$

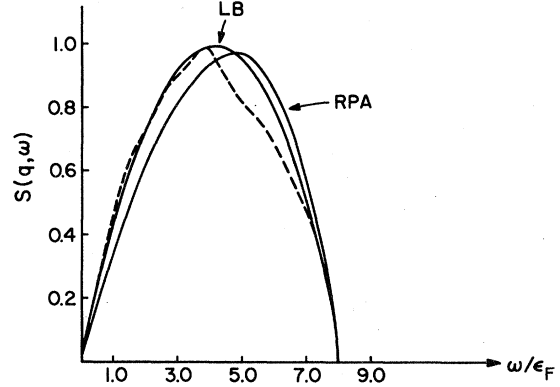
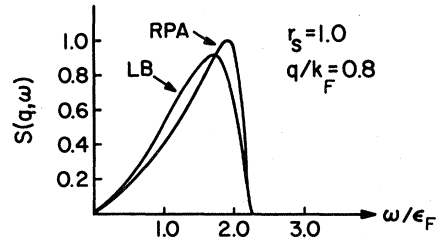


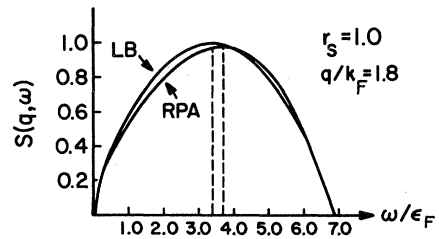
FIG. 7. Dynamic form factor for $r_s = 2.0$ and $q/k_F = 2.0$. The dashed line corresponds to the data taken for Be, $r_s = 1.8$, at $q/k_F = 2.1$ (see Ref. 6).

Indeed, for $q < q_c$, this is what one obtains when Eq. (48) is plugged into Eq. (49). This same behavior, in the long-wavelength limit for the static form factor, is present in the theory of the present paper. For momentum values below the cutoff we use Eq. (52) for the static form factor, and for momentum values above the cutoff we integrate Eq. (49) numerically.

The results for the dynamic form factor for various values of the momentum transfer and density are shown in Figs. 7–9. The results for the static form factor are given in the Figs. 10–12 along with the pair-correlation function defined below.



(a)



(b)

FIG. 8. Dynamic form factor calculated from RPA and the theory of the present paper at $r_s = 1.0$ and (a) $q/k_F = 0.8$ and (b) $q/k_F = 1.8$.

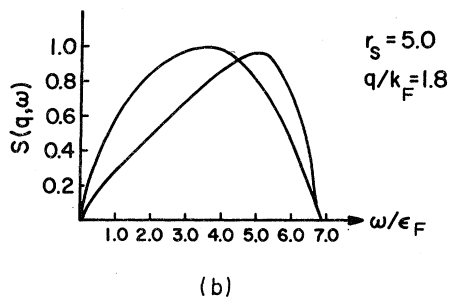
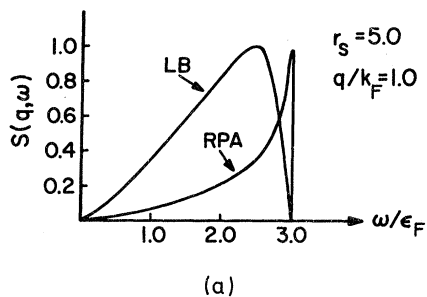


FIG. 9. Dynamic form factor for $r_s = 5.0$ for (a) $q/k_F = 1.0$ and (b) $q/k_F = 1.8$.

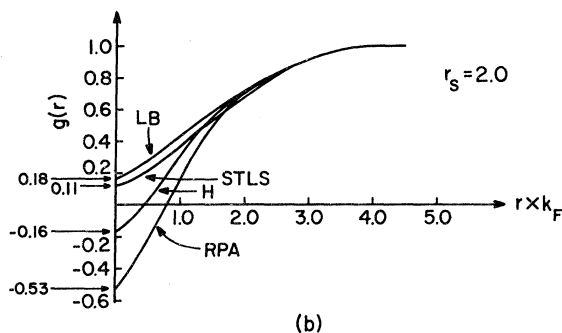
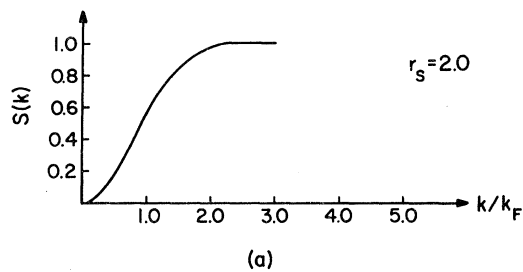


FIG. 11. (a) Static form factor $S(k)$ for $r_s = 2.0$. (b) The pair-correlation function $g(r)$ for $r_s = 2.0$.

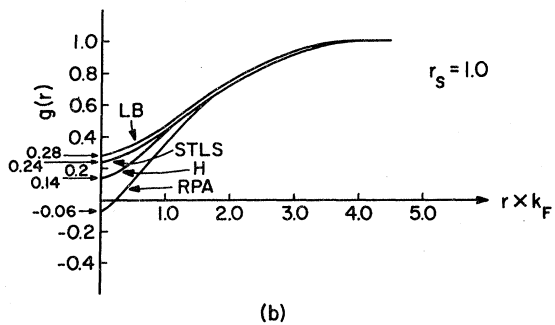
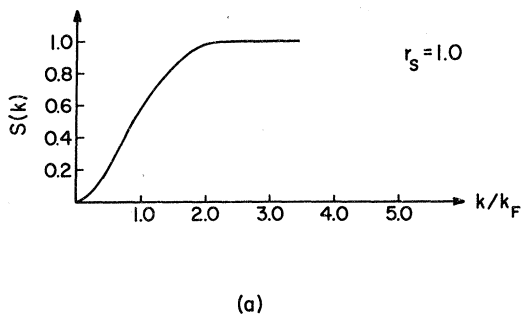


FIG. 10. (a) Static form factor $S(k)$ calculated from the present theory for $r_s = 1.0$. (b) The pair-correlation function $g(r)$ for $r_s = 1.0$. The values for STLS, RPA, and H are from Ref. 14. The LB curve is obtained by the procedure outlined in the present paper.

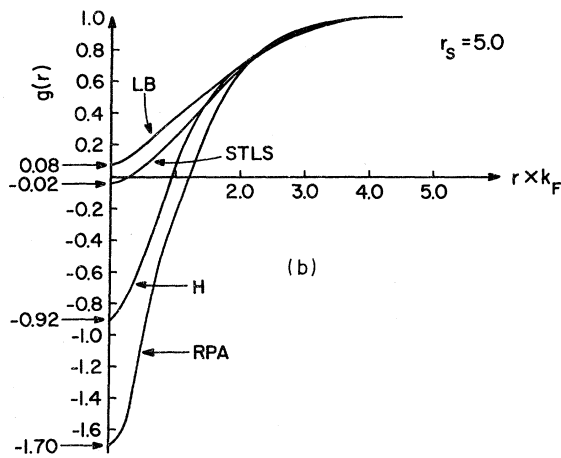
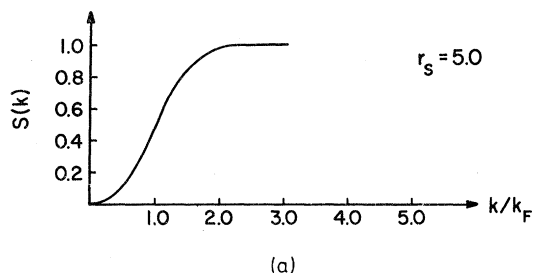


FIG. 12. (a) Static form factor $S(k)$ for $r_s = 5.0$. (b) The pair-correlation function $g(r)$ for $r_s = 5.0$.

E. Pair-correlation function

The instantaneous pair-correlation function $g(\vec{r})$ gives the probability of finding a particle at the point $\vec{R} + \vec{r}$ given that there is a particle at the point \vec{R} . It is related to the Fourier transform of the static form factor and is given by the equation

$$g(\vec{r}) = 1 + \frac{3}{2r} \int_0^\infty dq q \sin(qr) [S(\vec{q}) - 1]. \quad (53)$$

The results for our pair-correlation function are shown in the Figs. 10–12. We compare them with the results obtained in RPA, Hubbard's approximation, and with the results of Singwi *et al.* (STLS).¹ One of the things we note is that our $g(\vec{r})$ does not go negative for any values of the density no matter what the value of r is. Whereas in the other theories, $g(\vec{r})$ becomes negative for small r at low densities. That our $g(\vec{r})$ remains positive for small r at all densities is clearly a consequence of the short-range correlations we have built into the electron gas, since we employ here the same type of formalism as the other theories, but with a different effective interaction.

If we compare the results found for $g(\vec{r})$ in this paper and the original paper of Lowy and Brown, we find that the pair-correlation functions are essentially the same. One of the differences is that our $g(\vec{r})$ is larger for small values of r . The reason is that in the paper of LB, the plasmon contribution for small separations is neglected. In our results, we have included the effects of the plasmons on the small- r values of our $g(\vec{r})$. If the plasmon contribution is left out, the results we obtain for $g(\vec{r})$ are the same. Since the results for $g(\vec{r})$ are the same for two different approaches used, it becomes clear that $g(\vec{r})$ remains positive because of the physics we built into the pair-correlation function and that it is not due to the calculational scheme used.^{17,18} (In the Lowy-Brown formalism, $g(\vec{r})$ was expressed as the absolute value squared of the ratio of correlated to uncorrelated wave functions and was necessarily positive; here we employ a formalism which can easily give negative values of $g(\vec{r})$, depending upon the effective interaction.)

IV. SUM RULES

Sum rules provide a check on the consistency of a given theory of the electron gas. There are four sum rules for the electron gas that we can express in terms of the dynamic form factor and the dielectric response function³:

$$\int_0^\infty d\omega \omega S(\vec{q}, \omega) = \frac{\rho q^2}{2m}, \quad (54a)$$

$$\lim_{q \rightarrow 0} \int_0^\infty d\omega \frac{S(\vec{q}, \omega)}{\omega} = \frac{q^2}{8\pi e^2}, \quad (54b)$$

$$\int_0^\infty d\omega \omega S(\vec{q}, \omega) |\epsilon(\vec{q}, \omega)|^2 = \frac{\rho q^2}{2m}, \quad (54c)$$

and

$$\lim_{q \rightarrow 0} \int_0^\infty d\omega \frac{S(\vec{q}, \omega)}{\omega} |\epsilon(\vec{q}, \omega)|^2 = \frac{\rho}{2m s^2} \quad (54d)$$

The s^2 of Eq. (54d) is the square of the isothermal sound velocity in the electron gas.

Equation (54a) is the f -sum rule and is a consequence of particle conservation. The f -sum rule can be obtained from the equation of motion of the density fluctuations operator ρ_q . The derivation of this rule depends upon whether the density fluctuation operator commutes with the interaction part of the Hamiltonian. In our theory, we have an effective Hamiltonian given in second quantization as

$$H_{\text{eff}} = \sum_p \epsilon_p a_p^\dagger a_p + \frac{1}{2} \sum_{p, k, q} t^{\text{loc}}(q) a_{p+q}^\dagger a_{k-q}^\dagger a_k a_p. \quad (55)$$

The t -matrix in Eq. (55) is a local operator and it commutes with the density fluctuation operator. The ϵ_p are just the free-particle energies given by $\epsilon_p = p^2/2m$. Since ρ_q commutes with our interaction term the f -sum rule must be satisfied in our theory.

For momentum values below the cutoff, plasmons make the dominant contribution to the dynamic form factor. Thus, for $q < q_c$, plasmons exhaust the f -sum rule. For momenta greater than the cutoff, Eq. (54a) was integrated numerically and the sum rule was satisfied exactly (where *exactly* means that it was satisfied within the range of numerical error introduced by the integration).

The second sum rule Eq. (54b) is the perfect screening sum rule. This rule is satisfied exactly. The reason for this is that our effective interaction $t_{ph}^{\text{loc}}(q)$ goes to the Coulomb interaction $v(q)$ as $q \rightarrow 0$, so that in this limit the plasmons, etc. in our theory become identical with those in RPA.

The third sum rule is called the conductivity sum rule. This sum rule follows from the f -sum rule and the analytic properties of $\epsilon(\vec{q}, \omega)$. By direct numerical computation, this sum rule was also found to be satisfied exactly, indicating that we have not violated the known analytic behavior of $\epsilon(\vec{q}, \omega)$.

The sum rule of Eq. (54d) was checked by LB and it was found to be violated for all densities. A consistent treatment of the compressibility has proved to be difficult in the papers of Singwi *et al.*¹ and in LB (Ref. 2). Vashishta and Singwi¹⁴ fixed matters up by taking functional derivatives with respect to the density, but their method is not very

transparent.

We follow here the discussion of Pines and Nozières.³ The compressibility can be defined from the behavior of the screened response function

$$\lim_{q \rightarrow 0} \chi_{sc}(q, 0) = -\rho/m s^2, \quad (56)$$

where s is the velocity of sound, and is directly related to the compressibility κ . For our purpose, the most useful way to express the relationship is

$$\kappa^{\text{free}}/\kappa = s^2/s_0^2, \quad (56a)$$

where κ^{free} is the compressibility and s_0 the sound velocity of the noninteracting gas. The screened response function, in the polarization approach, can be expressed in terms of the function $f(q)$ in the following way:

$$\chi_{sc}(q, \omega) = \frac{\Pi_0(\vec{q}, \omega)}{1 + (4\pi e^2/q^2)f(q)\Pi_0(\vec{q}, \omega)}. \quad (56b)$$

Since

$$\lim_{q \rightarrow 0} \Pi_0(\vec{q}, 0) = -k_F m / \pi^2, \quad (56c)$$

we have, in general, that

$$\chi_{sc}(\vec{q}, 0) \xrightarrow{q \rightarrow 0} \left(\frac{-k_F m}{\pi^2} \right) \left[1 + \frac{4\pi e^2}{q^2} f(q) \left(\frac{-k_F m}{\pi^2} \right) \right]^{-1}. \quad (56d)$$

Equations (56), (56a), and (56d) yield, in the LB approximation

$$\frac{\kappa^{\text{free}}}{\kappa} \xrightarrow{q \rightarrow 0} 1 + \left(\frac{k_F m}{\pi^2} \right) \bar{t}_{ph}^{\text{loc}}(q). \quad (56e)$$

Let us stress that Eq. (56d) is a very general expression in the polarization potential approach. In the LB approach, $\bar{t}_{ph}^{\text{loc}}(q)$ can be expanded for small q as

$$\bar{t}_{ph}^{\text{loc}}(q) \xrightarrow{q \rightarrow 0} \frac{4\pi e^2}{q^2} \left[1 + \frac{|\vec{q}|^2}{k_F^2} \gamma + O\left(\frac{|\vec{q}|^3}{k_F^3}\right) + \dots \right], \quad (56f)$$

so that

$$\frac{\kappa^{\text{free}}}{\kappa} = 1 + \gamma \left(\frac{k_{TF}^2}{k_F^2} \right) = 1 + \gamma \left(\frac{4\alpha}{\pi} \right) \gamma_s. \quad (56g)$$

More generally, an expansion of $(4\pi e^2/q^2)f(q)$ could be carried out to give a γ for any given polarization potential.

One can also determine the compressibility directly by differentiating the energy per particle with respect to the density, or equivalently with respect to r_s [see Eq. (5.128) of Ref. 3],

$$\frac{\kappa^{\text{free}}}{\kappa} = \frac{1}{6}(\alpha^2 \gamma_s^4) \frac{\partial^2 \epsilon(r_s)}{\partial r_s^2} - \frac{1}{3}(\alpha^2 \gamma_s^3) \frac{\partial \epsilon(r_s)}{\partial r_s}. \quad (57)$$

The value found for $\kappa^{\text{free}}/\kappa$ obtained by differentiat-

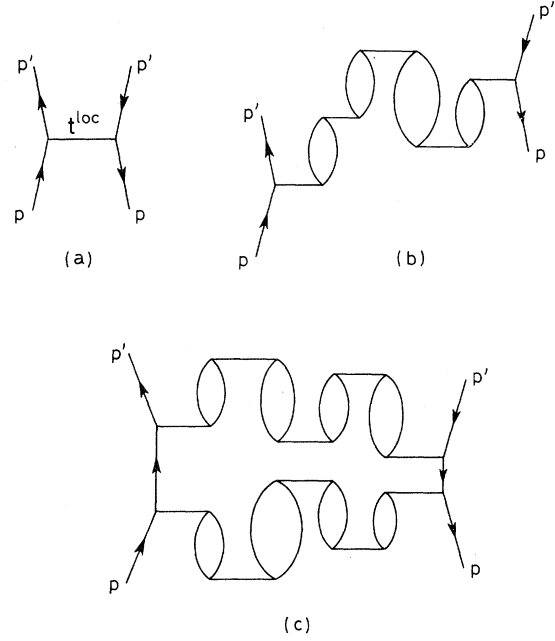


FIG. 13. Landau amplitude $f_{pp'}$, in (a) would be used to obtain the compressibility from Eq. (56g). The contributions to the compressibility from diagrams of the type shown in (b) and (c) would arise in the calculation of the compressibility from Eq. (57).

ing the LB energy is very different from the values given by Eq. (56g).

As is clear from the discussion in Chap. 5 of Ref. 3, the calculation of κ from Eq. (56g) can equivalently be expressed as calculating the compressibility from a Landau amplitude $f_{pp'}$, such as shown in Fig. 13(a). On the other hand, the double differentiation of the energy would, as discussed in Ref. 3, bring in the amplitudes of Figs. 13(b) and 13(c).

The LB calculations gave values of γ between -0.51 and -0.58 , whereas replacing $\bar{t}_{ph}^{\text{loc}}(q)$ in Fig. 13(a) by the Coulomb potential would give $\gamma = -0.25$. The larger value of $|\gamma|$ in the LB theory and in our calculation can be traced back to the averaging procedure for the t matrix, Eq. (21), which is inaccurate for momenta $\leq k_F$.

On the other hand, double differentiation of the energy gives results that are not very different from those obtained by differentiating the RPA energy. Thus, we believe that we understand the inconsistency between compressibilities calculated from Eq. (56) [which is equivalent to the compressibility sum rule, Eq. (54d)] and the results from differentiating the calculated energy.

Our calculation could be extended using the formalism of Babu and Brown¹⁹ so as to remove the discrepancy, and this would give an improved treatment of the compressibility, although it would

be difficult to include the process of Fig. 13(c). In any case, our formalism is clearly designed to get the high- q behavior, $q \gg k_F$, correct. Moreover, any extensions should include a proper treatment of the effective mass m^* . Proper treatment of the effective mass would involve the inclusion of the current-density response.⁴ Each of these considerations are, however, outside the scope of the present paper.

Let us note that the γ one has in Eq. (56g) is the same γ one finds in the plasmon dispersion relation, Eq. (38). Thus, in a very simple way the compressibility and the plasmon dispersion are related. This relationship is a consequence of the use of a static interaction. Our t matrix, or equivalently our function $f(q)$, is a function only of the momentum transfer and not a function of the frequency. Clearly, since the limits of the dielectric function to obtain the compressibility and the plasmon dispersion are different, one would expect an additional factor in the limit for the plasmon dispersion arising from the frequency dependence of the interaction. The same expression of Eq. (56g) would result for the compressibility since ω is set equal to zero before the limit as $q \rightarrow 0$ is taken. However, to the extent that one can assume the interaction to be instantaneous, a measure of the plasmon dispersion would also be a measure of the compressibility.

For the pair-correlation function, we have an additional check on the consistency of our calculation. We have that²⁰

$$g(\vec{r}) = 1 + \frac{1}{\rho} \int \frac{d^3q}{(2\pi)^3} [S(\vec{q}) - 1] e^{i\vec{q} \cdot \vec{r}}. \quad (58)$$

If we take the Fourier transform of $g(\vec{r}) - 1$ this gives

$$\int d^3r [g(\vec{r}) - 1] e^{-i\vec{p} \cdot \vec{r}} = \frac{1}{\rho} [S(\vec{p}) - 1].$$

In the limit as $p \rightarrow 0$,

$$\lim_{p \rightarrow 0} \int d^3r [g(\vec{r}) - 1] e^{-i\vec{p} \cdot \vec{r}} = \int d^3r [g(\vec{r}) - 1],$$

and

$$\lim_{p \rightarrow 0} S(\vec{p}) = 0.$$

This yields

$$\int d^3r [g(\vec{r}) - 1] = \frac{-1}{\rho}. \quad (59)$$

For the higher densities ($r_s = 1, 2, 3$), we satisfied this rule within a few percent. For the larger densities ($r_s = 4, 5$) the error was 7% and 10%, respec-

tively. Most of this error is due to the errors involved in the small- q approximation for $S(q)$ and the numerical integration errors made in the calculation of $S(\vec{q})$ from $S(\vec{q}, \omega)$ at the momentum value where the plasmon just merges with the particle-hole continuum.

V. CONCLUDING REMARKS

In this paper, we have studied the effects of short-range correlations on the properties of an electron gas. Our approach was to construct a density-density response function from which we were able to study the properties of an electron gas at metallic densities. One of the quantities studied was the pair-correlation function. The method we used to calculate $g(r)$ was different from that used by LB, however, the results we found were essentially the same. The results turned out to be independent of the method used indicating that the physics was responsible for the result and not some artifact of the calculation.

The dynamic form factor we calculated can be compared with experiment. Recent experiments indicate that the dynamic form factor has more structure than any of the theories, including the present one, can explain. There is a feature of the experiments that our theory might be used to explain. In a paper by Platzman and Eisenberger,⁷ it was found that the peak in the scattering cross section occurred at a lower value of the energy than predicted by the RPA. Platzman and Eisenberger suggested that this may in fact be due to short-range correlations in the static form factor. We see very clearly that this is what happens when short-range correlations are included in the electron gas since this leads to a plasmon energy that is lower than the plasmon energy of RPA, although this downward displacement is not all due to the high- \vec{q} behavior of the effective interaction in our theory. A comparison with some experimental results is shown in Fig. 8.

In conclusion, we feel that the theory presented in this paper gives a rather satisfactory microscopic description of the short-range correlations in the electron gas.

ACKNOWLEDGMENTS

We would like to thank Dr. D. N. Lowy for discussions in the initial phases of this work. We would also like to thank Professor Alpo Kallio and Dr. R. Machleidt for their advice. We have enjoyed many critical insights of Professor David Pines. This work was supported in part by U.S. ERDA Contract No. AT(11-1)-3001.

- ¹K. S. Singwi, A. Sjölander, M. P. Tosi, and R. H. Land, Phys. Rev. B 1, 1044 (1970); K. S. Singwi and P. P. Tosi, Phys. Rev. 181, 784 (1969); K. S. Singwi, A. Sjölander, M. P. Tosi, and R. H. Land, Solid State Commun. 7, 1503 (1969); R. Lobo, K. S. Singwi, and M. P. Tosi, Phys. Rev. 186, 470 (1969); K. S. Singwi, M. P. Tosi, R. H. Land, and A. Sjölander, *ibid.* 176, 589 (1968).
- ²D. N. Lowy and G. E. Brown, Phys. Rev. B 12, 2138 (1975).
- ³David Pines and P. Nozières, *The Theory of Quantum Liquids* (Benjamin, New York, 1966), Vol. I.
- ⁴C. H. Aldrich, III, C. J. Pethick, and D. Pines, Phys. Rev. Lett. 37, 845 (1976); C. H. Aldrich, III, and D. Pines, J. Low Temp. Phys. 25, 677 (1976); C. H. Aldrich, III, C. J. Pethick, and D. Pines, *ibid.* 25, 691 (1976).
- ⁵P. E. Batson, C. H. Chen, and J. Silcox, Phys. Rev. Lett. 37, 937 (1976).
- ⁶P. M. Platzman and P. Eisenberger, Phys. Rev. Lett. 33, 152 (1974).
- ⁷P. M. Platzman and P. Eisenberger, Solid State Commun. 14, 1 (1974).
- ⁸B. L. Scott and S. A. Moszkowski, Ann. Phys. (N.Y.) 14, 107 (1961).
- ⁹G. E. Brown, *Many-Body Problems* (North-Holland, Amsterdam, 1972).
- ¹⁰Alpo Kallio (private communication).
- ¹¹One should note that since the polarization propagator $\chi(q, \omega)$ can be expressed in terms of the screened response function $\chi_{sc}(q, \omega)$ of Ref. 3, as follows:
- $$\chi(q, \omega) = \chi_{sc}(q, \omega) / [1 - (4\pi e^2/q^2)\chi_{sc}(q, \omega)],$$
- $\chi_{sc}(q, \omega)$ and $\Pi^*(q, \omega)$ are identical operators.
- ¹²J. Lindhard, K. Dan. Vidensk. Selsk. Mat. Fys. Medd. 28, 8 (1954).
- ¹³David Pines, *The Many-Body Problem* (Benjamin, Reading, Mass., 1962), p. 205.
- ¹⁴P. Vashishta and K. S. Singwi, Phys. Rev. B 6, 875 (1972).
- ¹⁵Alexander L. Fetter and J. D. Walecka, *Quantum Theory of Many-Particle Systems* (McGraw-Hill, New York, 1971).
- ¹⁶D. F. Dubois, Ann. Phys. (N.Y.) 7, 174 (1959).
- ¹⁷B. I. Lundqvist, Phys. Kondens. Mat. 6, 193 (1967).
- ¹⁸T. P. Fishlock and J. B. Pendry, J. Phys. C 6, 1909 (1973). The approach used by the present authors is similar to that used by Fishlock and Pendry. The values we found for the pair-correlation function at $r=0$, $g(0)$ compare favorably with the results found by Fishlock and Pendry. This is a further confirmation of our claim that the short-range correlation we built into $g(r)$ are significant at short distances.
- ¹⁹S. Babu and G. E. Brown, Ann. Phys. (N.Y.) 78, 1 (1973).
- ²⁰To obtain this expression, terms of order $1/\rho V$, where V is the volume and ρ is the density of the system, are neglected. Retention of these makes the right-hand side of Eq. (59) zero. Such terms, however, will make no difference in expressions such as Eqs. (53) and (58); they come in only when the integration over volume is performed in Eq. (59).